

Infrared Photodissociation Spectra of Acrylonitrile Cluster Ions

Masahiko Ichihashi,^{†,‡} Yasuhiro Sadanaga,^{‡,§} and Tamotsu Kondow^{*,†,‡}

Cluster Research Laboratory, Toyota Technological Institute, East Tokyo Laboratory, Genesis Research Institute, Inc., 717-86 Futamata, Ichikawa, Chiba 272-0001, Japan, and Department of Chemistry, School of Science, The University of Tokyo, Bunkyo-ku, Tokyo 113-0033, Japan

Received: June 17, 1998

A coaxial infrared laser–ion beam photoabsorption spectrometer was constructed for the measurement of the vibrational spectrum of an acrylonitrile cluster cation, $(\text{CH}_2\text{CHCN})_n^+$ ($n = 3–10$), by detecting photodissociation products of the cluster ion in the wavenumber range of 925–1090 cm^{-1} . All the spectra measured in this n -range have an intense peak at 970 cm^{-1} , which is associated with a $\text{C}=\text{C}-\text{H}$ out-of-plane vibration of an acrylonitrile molecule in the cluster ion. The comparison of the spectra with an ab initio calculation shows that the cluster ion consists of a dimer ion core solvated with neutral acrylonitrile molecules. On the other hand, the acrylonitrile cluster anions did not exhibit any optical absorption in the wavenumber range studied. This finding is consistent with our previous result that intracluster polymerization takes place when an electron is attached onto a neutral cluster of acrylonitrile.

1. Introduction

The density of states in a cluster is sufficiently high that the energy introduced into the cluster flows with relative readiness among its internal modes, but it is not sufficiently high that the energy tends to be concentrated in a particular mode in a relatively short time period. Accordingly, the energy introduced to the cluster tends to be concentrated in an intermolecular mode associated with rupture of its intermolecular bond. This feature facilitates the measurement of the photodissociation spectrum of the cluster in an infrared region; a photon possessing only a marginal energy for its bond rupture causes the cluster to dissociate due to sufficient energy deposition to the particular intermolecular mode leading to the dissociation. In this case, the photodissociation spectrum turns out to be equivalent to the optical absorption spectrum since the cluster is considered to dissociate fully when it absorbs one photon.

By taking advantage of this specific feature, vibrational structures of neutral and ionic clusters have been investigated.^{1–8} These studies have unveiled the fundamental features of cluster structures and dynamics related to what finite many-body systems themselves possess. The size-dependent photodissociation spectra of several cluster ions have been reported in the wavenumber range of a line-tunable CO_2 laser. For example, the vibrational spectrum of $\text{Cs}^+(\text{CH}_3\text{OH})_n$ has revealed that 10 methanol molecules form the first solvation shell around Cs^+ .³ The first solvation shell is so rigid that its structure does not change appreciably with addition of solvent molecules to it, which contribute to form the next solvation shell. Several binary cluster ions, such as $\text{SF}_6\cdot\text{Ar}_n^+$, have been investigated.⁵ In the wavenumber range of 910–970 cm^{-1} , $\text{SF}_6\cdot\text{Ar}_n^+$ ($n \leq 40$) exhibits sharp triple peaks associated with the triply degenerated ν_3 mode of SF_6 , probably because $\text{SF}_6\cdot\text{Ar}_n^+$ has rigid and ordered structure. It also has been concluded that $\text{SF}_6\cdot\text{Ar}_n^+$ has one neutral SF_6 molecule as the chromophore, along with the

positive charge on the argon cluster, while the SF_6 molecule is not located at the center of the cluster ion. Recently, we have measured the optical absorption spectrum of $\text{NH}_4^+(\text{NH}_3)_{n-1}$ ($n = 6–9$), having a high internal energy in the wavenumber range of 1045–1091 cm^{-1} , and have found a collective vibrational mode related to the ν_2 vibrations of NH_3 molecules in the second solvation shell.⁶ We have concluded that the first solvation shell is completed by four ammonia molecules on the basis of the measurement of its optical absorbance. Vibrational spectroscopy provides important information on the cluster structure, such as the number of the constituent molecules of the ion core and each solvation shell.

In this report, we describe the optical absorption spectra of acrylonitrile cluster cations and anions by use of a coaxial infrared laser–ion beam spectrometer developed for the present experiment. The results showed that the cluster cations consist of a dimer ion core solvated with neutral acrylonitrile molecules, while the anions are polymer anions formed by intracluster anionic polymerization and have no distinct absorption band in the wavenumber range studied.

2. Experimental Section

Figure 1 shows a schematic drawing of the coaxial infrared laser–ion beam photoabsorption spectrometer used in the present experiments. As described in detail previously,^{9,10} a mass-selected ion beam source consists of a supersonic nozzle having a platinum aperture (30 μm) and a conical skimmer. Argon gas at a stagnation pressure of 2.2 atm containing ≈ 100 Torr of acrylonitrile (AN, CH_2CHCN) vapor was expanded through the nozzle into a vacuum chamber. Commercially available acrylonitrile was used without any further purification. Acrylonitrile clusters formed in the free jet expansion were skimmed and collimated in the second chamber. The clusters were ionized by electron impact in a housing mounted in the third chamber, where three concentric cylindrical grids and four pieces of helical filaments in a rectangular arrangement are mounted; the grids are made of stainless steel mesh with a transmittance of 80%, and the filaments are made of thoriated tungsten wire

[†] Toyota Technological Institute.

[‡] The University of Tokyo.

[§] Present address: Research Center for Advanced Science and Technology, The University of Tokyo, Meguro-ku, Tokyo 153-0041, Japan.

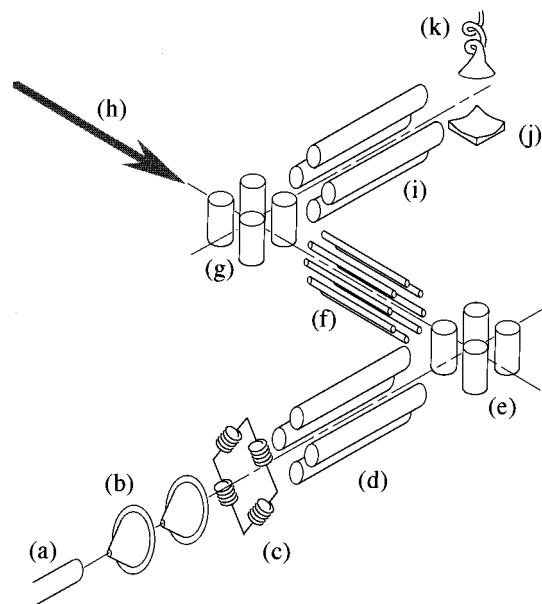


Figure 1. Schematic drawing of the coaxial infrared laser-ion beam photoabsorption spectrometer. No einzel lenses are drawn for clarity from the other part of the apparatus. (a) Nozzle, (b) skimmer, (c) electron gun, (d and i) quadrupole mass filter, (e and g) quadrupole deflector, (f) octopole ion guide, (h) CO₂ laser, (j) ion conversion dynode, and (k) secondary electron multiplier.

of 0.15-mm diameter. Electrons emitted from the filaments biased at a desired voltage (≈ 40 V typically) are admitted into the central grid, where the clusters are ionized by collision with the electrons.

Ionic species thus produced were focused by two sets of einzel lenses with deflectors and extracted through an entrance slit into a quadrupole mass filter (Extrel, 162-8) installed in the fourth chamber. The ion beam after the quadrupole mass filter was focused by a set of ion lenses and deflected in one quadrupole deflector by 90° so as to merge in an octopole ion beam guide (50 cm in length) with a CO₂ laser beam. The ion beam was found to be fully covered with the CO₂ laser beam in the interaction region of the ion guide until it was deflected off by the other quadrupole deflector. The quadrupole deflectors used are similar to that reported in ref 11 but differ slightly in dimensions and design.

The octopole ion guide (OPIG) consists of eight cylindrical molybdenum rods of 3.0-mm diameter, which are positioned on a 12-mm-diameter circle. Radio frequency field (7.2 MHz, ≈ 200 V) was supplied to the rods so as to prepare a radial potential well inside the OPIG.¹²⁻¹⁴ The generated potential well has a fairly flat bottom and steeply rising walls, which trap the ion very efficiently in it, and the ions (≈ 10 eV or less) traveling along the axis of the OPIG do not change its translational energy. A radio frequency power supply for preparing the potential well is a commercially available high-frequency transceiver, which is interfaced with a resonant LC circuit composed of a load capacitance of the OPIG and an external induction coil.

The output of a continuous wave line-tunable CO₂ infrared laser (Edinburgh Instruments, PL5) was introduced coaxially into the OPIG in the wavenumber range from 925 to 1090 cm^{-1} . The laser beam passing through an aperture 5 mm in diameter was admitted coaxially through a ZnSe window into the OPIG in the vacuum chamber and was allowed to pass through a Ge window. The power of the laser beam was always monitored to be in the range of 4 W by a power meter (Coherent, Field

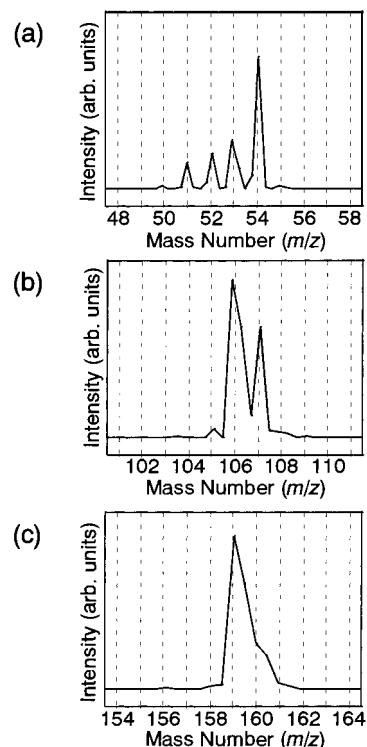


Figure 2. Mass spectra of acrylonitrile cluster cations. In panel a, the peaks at $m/z = 53$ and 54 are associated with $(\text{AN})^+$ and $(\text{AN})\text{H}^+$, respectively; in panel b, the peaks at $m/z = 106$ and 107 are associated with $(\text{AN})_2^+$ and $(\text{AN})_2\text{H}^+$, respectively; and in panel c, the peaks at $m/z = 159$ and 160 are associated with $(\text{AN})_3$ and $(\text{AN})_3\text{H}^+$, respectively.

Master) located outside the exit Ge window, where the transmittance of the Ge window is taken into account for evaluating the laser power in the OPIG. As the diameter of the laser beam is larger than that of the ion beam in the radial potential well of the OPIG, all the ions in the OPIG are considered to be irradiated fully by the laser beam. This complete overlap of the ion and the laser beams enables us to determine the absolute photodissociation cross sections.

The ions after passing through the OPIG were deflected by the second quadrupole deflector, focused by a set of ion lenses, and extracted through an entrance slit into a quadrupole mass filter in the fifth chamber. An ion conversion dynode made of stainless steel was bombarded with the mass-selected ions, and charged particles sputtered from the dynode were detected by a secondary electron multiplier (Murata, Ceratron EMS-1081B). The electrical signal from the multiplier was amplified, discriminated, and processed by a microcomputer (NEC, PC-9801RA).

3. Results

Figure 2 shows typical mass spectra of the parent cluster ions from the source in the m/z range between 48 and 164. As shown in Figure 2, the protonated cluster ions, $(\text{AN})_n\text{H}^+$, are well separated from the nonprotonated cluster ions, $(\text{AN})_n^+$. The spectrum of the parent cluster ions larger than the trimer ion is not shown, as the protonated cluster ions, $(\text{AN})_n\text{H}^+$, diminish for $n \geq 3$. After elimination of $(\text{AN})_n\text{H}^+$, only $(\text{AN})_n^+$ was allowed into the region where the measurement is performed. Typical mass spectra of daughter cluster ions produced from $(\text{AN})_{10}^+$ with and without laser radiation are shown in Figure 3a and b, respectively. The daughter ion, $(\text{AN})_9^+$, is observed even without laser radiation, because of unimolecular dissocia-

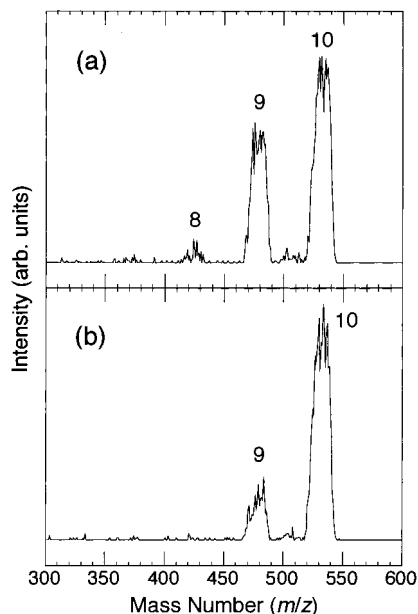
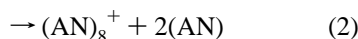
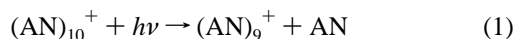
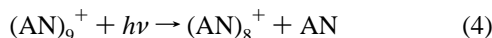
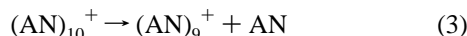


Figure 3. Mass spectra of the ions produced from $(AN)_{10}^+$ with and without the laser beam (panels a and b, respectively). The wavenumber and the power of the CO_2 laser used are 975 cm^{-1} and 4.1 W , respectively. Peak broadening is attributed to low resolution of the mass filter for high transmittance.

tion of the parent cluster ion. Evidently, the parent cluster ion gains a large amount of internal energy during its ionization. Upon irradiation of the laser, $(AN)_9^+$ and $(AN)_8^+$ were produced from the parent cluster ion, $(AN)_{10}^+$, and the unimolecularly dissociated ion, $(AN)_9^+$, respectively,



and/or



As the intensity of the daughter ion, $(AN)_9^+$, increases linearly with the laser power, this photodissociation should be a single-photon process.

The photodissociation cross section, σ , was determined from depletion of the intensity of the parent cluster ion by laser irradiation as

$$\sigma = \frac{\pi r^2 h\nu}{Pt} \log \frac{I_0}{I} \quad (5)$$

where I and I_0 represent the relative intensities of the parent cluster ion with and without laser radiation, t is the interaction time, $h\nu$ is the photon energy, r is the radius of the laser spot, and P is the laser power. A photodissociation spectrum was obtained by measuring the photodissociation cross section as a function of the wavenumber of the CO_2 laser.

Figure 4 shows the photodissociation spectrum of $(AN)_{10}^+$ in the $925\text{--}1090\text{-cm}^{-1}$ region, where one intense peak is observed at about 970 cm^{-1} . This peak is associated with an out-of-plane vibration of a constituent acrylonitrile molecule because an isolated acrylonitrile molecule has two strong vibrational transitions at 953.5 and 971.0 cm^{-1} which are

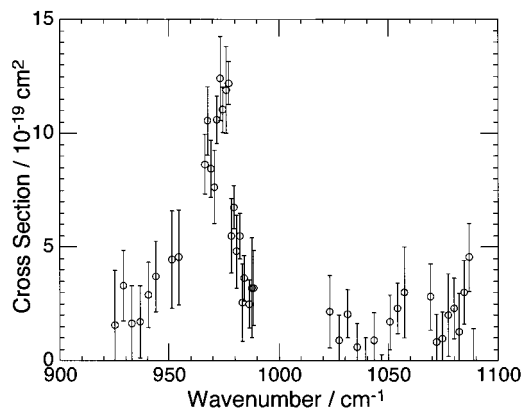


Figure 4. Photodissociation spectrum of $(AN)_{10}^+$ in the wavenumber range of $925\text{--}1090\text{ cm}^{-1}$.

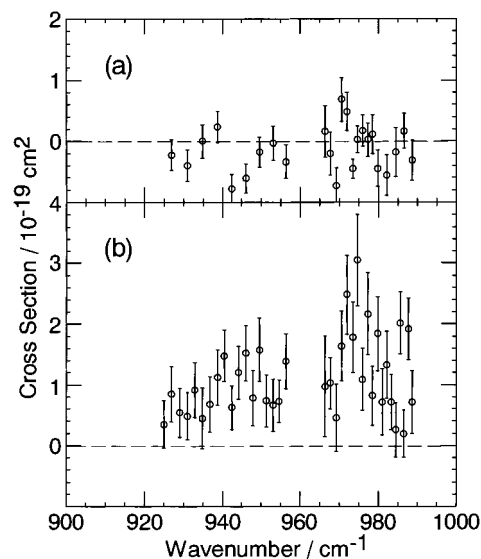


Figure 5. Photodissociation spectra of $(AN)_2^+$ and $(AN)_3^+$ in the wavenumber range of $925\text{--}990\text{ cm}^{-1}$ (panels a and b, respectively).

assigned to $C=C-H$ out-of-plane wagging and twisting modes of the vinyl group, respectively.^{15–17}

The photodissociation spectra of $(AN)_2^+$ and $(AN)_3^+$ are shown in Figure 5a and b, respectively. The spectrum of $(AN)_3^+$ has two peaks at ≈ 950 and $\approx 970\text{ cm}^{-1}$, which are related to the wagging and the twisting modes of an isolated acrylonitrile molecule, respectively. On the other hand, the spectrum of $(AN)_2^+$ does not exhibit any discernible peak in this wavenumber range.

The trimer ion, $(AN)_3^+$, is the smallest cluster ion whose spectrum exhibits a recognizable peak in the wavenumber range studied. The size evolution of the photodissociation spectrum is shown in Figure 6. As mentioned above, the spectrum of $(AN)_3^+$ has two peaks. As the cluster size increases, the peak at 970 cm^{-1} becomes broader and larger, while that at 950 cm^{-1} tends to be smaller, and only one large peak at 970 cm^{-1} is discernible above the size of six. Actually, the 970-cm^{-1} peak is observed in the IR absorption spectrum of liquid acrylonitrile and corresponds to CH_2 , CH out-of-plane vibration of a constituent acrylonitrile molecule. The line-broadening in the present spectrum is attributable to a structural change caused by a high internal energy in the parent cluster ion. Therefore, this peak in the spectrum was fitted by a Gaussian function. The optical absorbance was obtained as the integral of the peak. The optical absorbance of $(AN)_n^+$ at about 970 cm^{-1} was found to increase linearly with the cluster size, as shown in Figure 7.

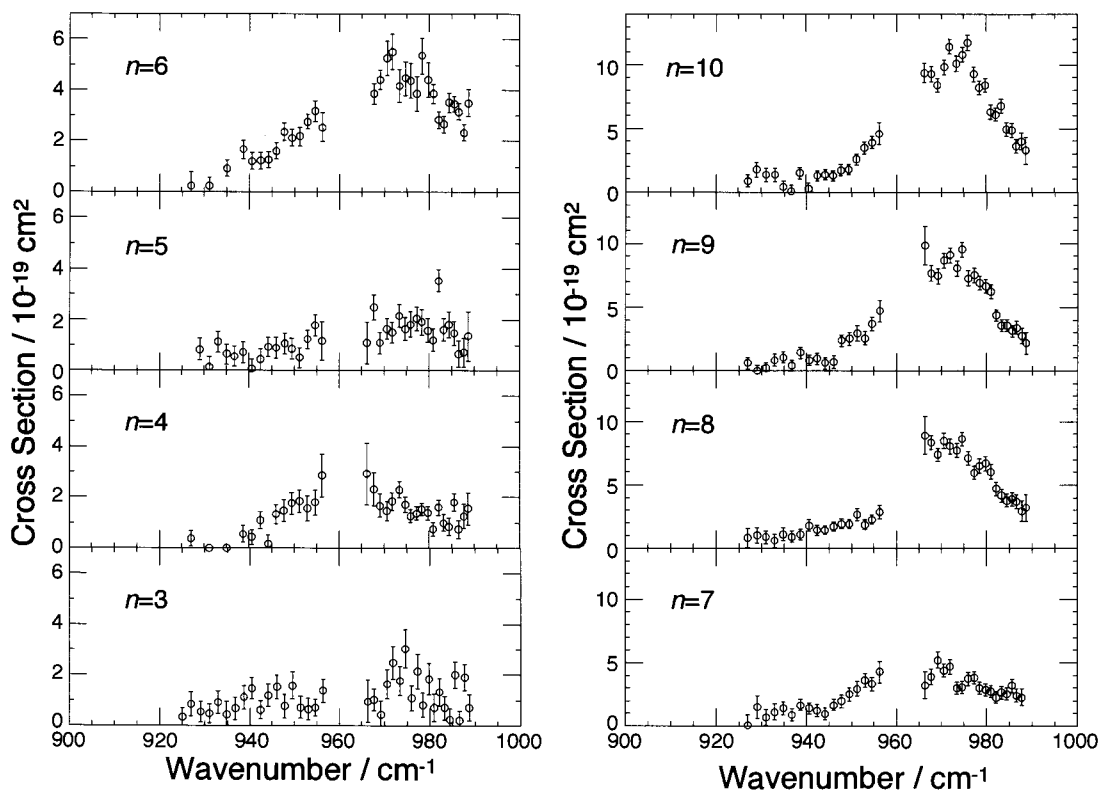


Figure 6. Photodissociation spectra of $(AN)_n^+$ ($n = 3-10$) in the wavenumber range of 925–990 cm^{-1} .

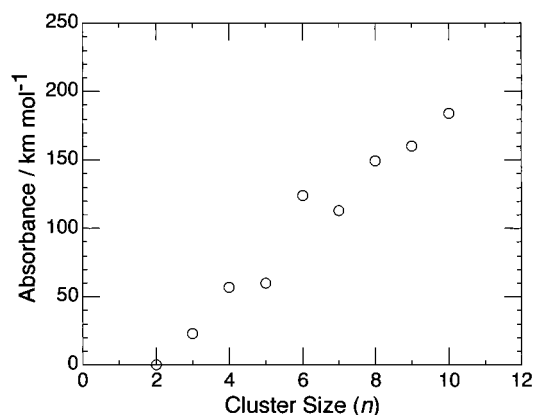


Figure 7. Optical absorbance of $(AN)_n^+$. The optical absorbance was obtained as the integral of the Gaussian function fitted to the peak profile in the photodissociation spectrum.

4. Discussion

4.1. Structures of Dimer and Trimer Cations. The optimized structures and the wavenumbers of harmonic vibration of $(AN)_2^+$ and $(AN)_3^+$ were calculated by use of Gaussian 94 at the MP2/6-31G level.¹⁸ The optimized geometries of $(AN)_2^+$ and $(AN)_3^+$ are shown in Figure 8. One constituent molecule at the right-hand side of $(AN)_2^+$ shown in Figure 8 has almost the same structure as that of an isolated acrylonitrile molecule. The Mulliken population analysis reveals that this constituent molecule possesses a charge of 0.31. The rest of the charge is distributed on the other molecule, whose structure differs markedly from that of the isolated molecule. The trimer cation, $(AN)_3^+$, has a positive charge localized exclusively on two of its constituent molecules; i.e., the trimer cation consists of one dimer ion core and one neutral solvent molecule. The dimer ion core has almost the same structure as that of the isolated $(AN)_2^+$.

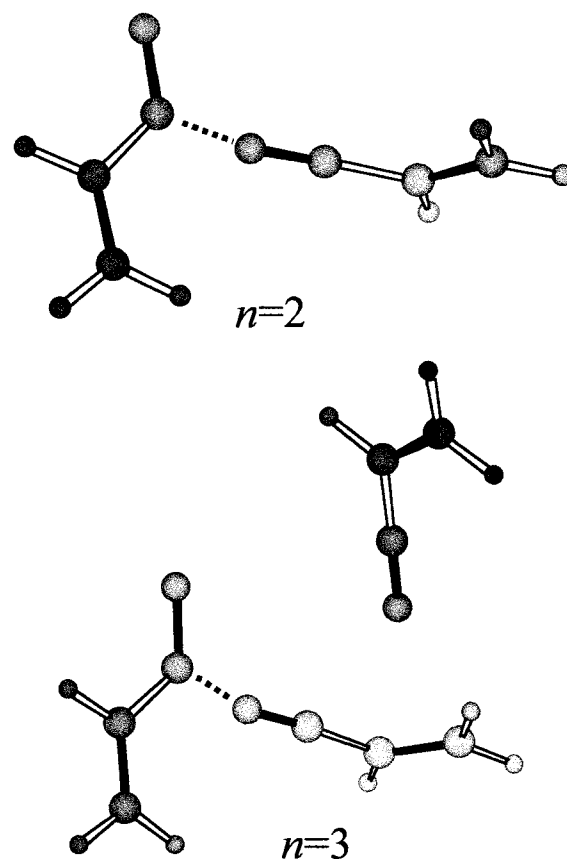


Figure 8. Ab initio optimized geometries of $(AN)_2^+$ and $(AN)_3^+$ at the MP2/6-31G level.

The wavenumbers of the harmonic vibrations of $(AN)_2^+$ and $(AN)_3^+$ were calculated. The absolute values of the calculated wavenumbers were not sufficiently accurate that the calculated values were scaled by comparison of the calculated values of

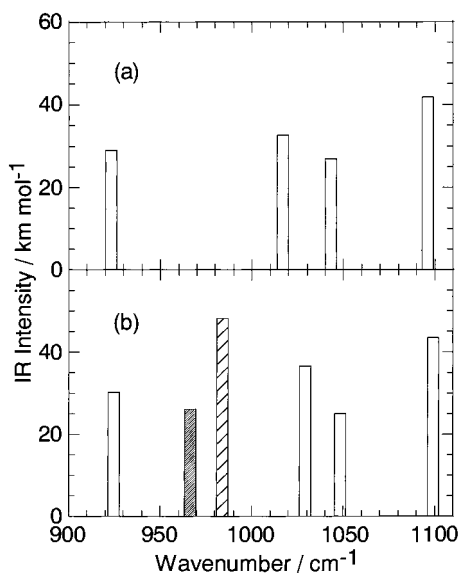


Figure 9. Ab initio wavenumbers of harmonic vibrations of $(\text{AN})_2^+$ (panel a) and $(\text{AN})_3^+$ (panel b) at the MP2/6-31G level. The bars hatched thickly and thinly show the wagging and the twisting modes of the solvent acrylonitrile molecule, respectively.

an isolated acrylonitrile molecule with the corresponding experimental ones. The ab initio calculation for the wavenumbers of the wagging and the twisting modes of the acrylonitrile molecule was performed at the same calculation level as that employed for the cluster ion calculation. The calculated wavenumbers were 964.6 (wagging) and 1017.6 cm^{-1} (twisting), while the experimental ones are 953.5 (wagging) and 971.0 cm^{-1} (twisting).¹⁷ The ratios of the experimental wavenumbers to the calculated ones were 0.9885 and 0.9542 for the wagging and the twisting modes, respectively. The averaged value of the two ratios (0.9713) was employed as the scaling factor; the wavenumbers obtained by the calculation were always multiplied by the scaling factor, so as to obtain the calculated wavenumbers with correction for comparison with the experimental ones. The calculated wavenumbers with correction (hereafter called the calculated wavenumbers) thus obtained are shown in Figure 9. In the 900–1100- cm^{-1} range, the isolated acrylonitrile molecule has two vibrational modes (wagging and twisting modes), while the dimer cation has four vibrational modes. On the other hand, the trimer cation has all of the vibrational modes inherent to the isolated acrylonitrile molecule and the dimer ion core. They are the wagging and the twisting modes of the neutral acrylonitrile molecule and the vibrational modes of the dimer ion core, which are well separated from each other. As is the case with $\text{NH}_4^+(\text{NH}_3)_{n-1}$,⁶ good separation of the vibrational modes of the ion core and the solvent molecules is one of the essential features of such solvated cluster ions.

By comparison of the calculated wavenumbers of the wagging (966.7 cm^{-1}) and the twisting (983.9 cm^{-1}) modes with the observed spectrum of the trimer cation, one concludes that the 950- and the 970- cm^{-1} peaks originate from the wagging and the twisting modes of the neutral solvent molecule in the trimer cation. The calculated infrared intensity of the twisting mode of the trimer cation is higher than that of the wagging mode. This result confirms that the intense and broad peak at 970 cm^{-1} is assigned to the twisting mode of the solvent molecule in the trimer cation.

4.2. Structure of Cluster Cations. As mentioned in the previous section, the trimer cation possesses one dimer ion core, $(\text{AN})_2^+$, which is solvated with one neutral acrylonitrile

molecule. The structure of the tetramer cluster cation, $(\text{AN})_4^+$, was also calculated by use of Gaussian 94 at the MP2/6-31G level, where the initial structure of $(\text{AN})_4^+$ is set to have an optimized trimer cation and a neutral AN molecule. A stable structure of $(\text{AN})_4^+$ calculated shows that $(\text{AN})_4^+$ thus obtained consists of a dimer ion core and two solvent molecules. Conceivably, a larger cluster cation, $(\text{AN})_n^+$ ($n \geq 3$), has a similar structure: one dimer ion core is solvated with $(n - 2)$ acrylonitrile molecules. As described in the previous section, the chromophore in the trimer cation is its solvent molecule, which has the wagging and twisting vibrational modes at about 950 and 970 cm^{-1} , respectively. Therefore, the proportionality of the optical absorbance with $(n - 2)$ implies that $(\text{AN})_n^+$ contains $(n - 2)$ neutral chromophores, that is, $(n - 2)$ neutral acrylonitrile molecules. As the peak itself does not shift with the number of the solvent molecules, the solvent molecules do not seem to interact significantly with each other. No significant peak shift is observed as well for the corresponding peak of acrylonitrile molecules in a rare gas matrix,^{15,16} where a peak assignable to the vibrations of aggregates appears at 983 cm^{-1} at a large concentration in the matrix in addition to the peaks of the wagging and the twisting modes of the isolated molecules. This finding shows that formation of hydrogen bonds between the molecules causes a significant shift in the vibrational wavenumber but that the vibrational wavenumber does not depend on the cluster size. In the case of the cluster cation, interaction between the constituent solvent molecules by hydrogen bond formation affects the shift of the wavenumber much less than the interaction between the ion core and a solvent molecule.

4.3. Cluster Anions. An attempt was also made to measure the photodissociation spectra of the cluster anions, $(\text{AN})_n^-$ ($n \leq 11$), but no intense absorption was observed in the 925–1090- cm^{-1} region. If the cluster anion has appreciable optical absorption in the wavenumber region, it should dissociate, because the anion has enough internal energy for unimolecular dissociation. No absorption is consistent with the result that the intracuster reaction proceeds due to electron attachment on a neutral acrylonitrile cluster; the constituent acrylonitrile molecules are polymerized by the electron attachment (anionic polymerization).^{19–22}

Acknowledgment. The ab initio calculation was performed by NEC HSP and HPC of the Computer Center, Institute for Molecular Science, Okazaki National Research Institutes. The present work was supported by the Cluster Science Project of Genesis Research Institute, Inc., and a Grant-in-Aid for Scientific Research in Priority Areas by the Ministry of Education, Science and Culture of Japan.

References and Notes

- (1) Buck, U. *J. Phys. Chem.* **1994**, *98*, 5190.
- (2) Huisken, F.; Kaloudis, M.; Kulcke, A.; Laush, C.; Lisy, J. M. *J. Chem. Phys.* **1995**, *103*, 5366.
- (3) Draves, J. A.; Luthey-Schulten, Z.; Liu, W.-L.; Lisy, J. M. *J. Chem. Phys.* **1990**, *93*, 4589.
- (4) Weinheimer, C. J.; Lisy, J. M. *J. Chem. Phys.* **1996**, *100*, 15305.
- (5) Winkel, J. F.; Woodward, C. A.; Jones, A. B.; Stace, A. J. *J. Chem. Phys.* **1995**, *103*, 5177.
- (6) Ichihashi, M.; Yamabe, J.; Murai, K.; Nonose, S.; Kondow, T. *J. Phys. Chem.* **1996**, *100*, 10050.
- (7) Johnson, M. S.; Kuwata, K. T.; Wong, C.-K.; Okumura, M. *Chem. Phys. Lett.* **1996**, *260*, 551.
- (8) Choi, J.-H.; Kuwata, K. T.; Haas, B.-M.; Cao, Y.; Johnson, M. S.; Okumura, M. *J. Chem. Phys.* **1994**, *100*, 7153.
- (9) Kondow, T. *J. Phys. Chem.* **1987**, *91*, 1307.
- (10) Mitsuke, K.; Kondow, T.; Kuchitsu, K. *J. Phys. Chem.* **1986**, *90*, 1552.
- (11) Farley, J. W. *Rev. Sci. Instrum.* **1985**, *56*, 1834.

- (12) Gerlich, D. *Adv. Chem. Phys.* **1992**, 82, 1.
- (13) Hanley, L.; Ruatta, S. A.; Anderson, S. L. *J. Chem. Phys.* **1987**, 87, 269.
- (14) Okuno, K. *J. Phys. Soc. Jpn.* **1986**, 55, 1504.
- (15) George, W. O.; Lewis, E. N.; Williams, D. A.; Maddams, W. F. *Appl. Spectrosc.* **1982**, 36, 592.
- (16) Reedy, G. T.; Ettinger, D. G.; Schneider, J. F.; Bourne, S. *Anal. Chem.* **1985**, 57, 1602.
- (17) George, W. O.; Hirani, P. K.; Lewis, E. N.; Maddams, W. F.; Williams, D. A. *J. Mol. Struct.* **1986**, 141, 227.
- (18) Frisch, M. J.; Trucks, G. W.; Schlegel, H. B.; Gill, P. M. W.; Johnson, B. G.; Robb, M. A.; Cheeseman, J. R.; Keith, T.; Petersson, G. A.; Montgomery, J. A.; Raghavachari, K.; Al-Laham, M. A.; Zakrzewski, V. G.; Ortiz, J. V.; Foresman, J. B.; Cioslowski, J.; Stefanov, B. B.; Nanayakkara, A.; Challacombe, M.; Peng, C. Y.; Ayala, P. Y.; Chen, W.; Wong, M. W.; Andres, J. L.; Replogle, E. S.; Gomperts, R.; Martin, R. L.; Fox, D. J.; Binkley, J. S.; Defrees, D. J.; Baker, J.; Stewart, J. P.; Head-Gordon, M.; Gonzalez, C.; Pople, J. A. *Gaussian 94*, Revision C.3; Gaussian, Inc.: Pittsburgh, PA, 1995.
- (19) Tsukuda, T.; Kondow, T. *J. Am. Chem. Soc.* **1994**, 116, 9555.
- (20) Ichihashi, M.; Tsukuda, T.; Nonose, S.; Kondow, T. *J. Phys. Chem.* **1995**, 99, 17354.
- (21) Fukuda, Y.; Tsukuda, T.; Terasaki, A.; Kondow, T. *Chem. Phys. Lett.* **1995**, 242, 121.
- (22) Fukuda, Y.; Tsukuda, T.; Terasaki, A.; Kondow, T. *Chem. Phys. Lett.* **1996**, 260, 428.